20pt

THERMAL MODEL PREDICTIONS OF ULTRASONIC LESION FORMATION

Michael C. Kolios, Michael D. Sherar and John W. Hunt
Department of Medical Biophysics
University of Toronto
Toronto, Ontario
Canada

ABSTRACT

Blood flow can effect temperature distributions of heated tissues. In this work the effects of microvascular cooling on temperature distributions during ultrasonic lesioning are examined. Microvascular cooling was assessed using two simple thermal models used in hyperthermia treatment planning: the Pennes Bioheat Transfer Equation (BHTE) and the scalar Effective Thermal Conductivity Equation (ETCE). The equations of heat transfer in perfused tissues were solved by finite differences in cylindrical coordinates. The extent of the lesioned tissue was determined by the accumulated thermal dose at each location. The size of the lesion was then calculated from the boundaries of the thermal isodose curves generated by the simulations. The model of bioheat transfer used can strongly influence simulation outcome. Even for short exposure times of ultrasonic heating, blood flow may be a significant determinant of the lesion shape and size.

NOMENCLATURE

c = specific heat capacity (J/kg-°C)
dr = grid spacing in the radial direction (m)
dz = grid spacing in the axial direction (m)
k = thermal conductivity (W/m-°C)
k_{eff} = scalar effective conductivity of tissue (W/m-°C)
r, z = radial and axial coordinates (m)
u(r) = velocity of blood (m/sec)
w = volumetric perfusion rate ($g/cm^3/s$)
P = volumetric power deposition rate (W/m^3)
T = temperature (°C)
R = empirical parameter in thermal dose equation 3
α = best fit parameter equating perfusion and effective conductivity $(g/cm^3\text{-}s)^{-1}$
δ = blood vessel diameter (m)
ρ = density (kg/m^3)

subscripts
art = arterial
avg = average

INTRODUCTION

Focussed ultrasound has been used to produce lesions in tissues for the treatment of various pathologies (ter Haar *et al.* 1991). It is thought that the primary mechanism of lesion damage is thermal in nature (NCRP 1992). Thus the time-temperature history of the heated tissues can be used to predict the extent of lesion formation. Blood flow may play an important role since it can have strong cooling effects in the heated field. The effects can be divided into large (or thermally significant) vessel cooling and the collective effect of smaller vessels. Vascular models are used to model the effects of large vessels and continuum models are used for the effects of the numerous smaller vessels. This work examines the influence of continuum thermal models on simulated

temperature profiles of ultrasonic lesioning and in turn, lesion outcome. Based on the time-temperature curves, predictions are made as to the extent of the lesioned tissue.

Intermediate and small sized vessels, due to their number and complex geometry, cannot be accounted for individually in thermal models. Several models have been used to account for the effects of microvascular flow on the temperature distribution of heated tissues. In these models, the contributions of many blood vessels are averaged in order to predict a local average temperature (Baish 1994). Two such models have been used for hyperthermia treatment planning: the Pennes Bioheat Transfer Equation (BHTE) (Pennes 1948; Roemer 1991) and the scalar Effective Thermal Conductivity Equation (ETCE) (Weinbaum *et al.* 1984; Lagendijk 1990). In the BHTE it is assumed that blood reaches the capillaries at the temperature of the supply vessels and thermally equilibrates with the surroundings instantaneously, exiting the veins at the local average temperature (Pennes 1948). Microvascular flow thus acts as an isotropic heat sink. In the ETCE it is assumed that blood equilibration occurs at higher levels of the circulation, and the the collective effect of these vessels can be modeled as an enhanced conductivity of tissue (Weinbaum *et al.* 1984). If the vascular tree is isotropic, then the effective conductivity tensor can be simplified to a scalar. Arkin *et al.* (1994) have recently reviewed these and other existing models. Recent experimental hyperthermic data supports both models discussed (Moros *et al.* 1993; Crezee and Lagendijk 1990).

TEMPERATURE CALCULATIONS

A finite difference algorithm was used to solve the BHTE and ETCE in cylindrical coordinates. In brief, the equation solved was:

$$\rho_t c_t \frac{\partial T}{\partial t} = k_{eff}\left(\frac{\partial^2 T}{\partial^2 r} + \frac{1}{r}\frac{\partial T}{dr} + \frac{\partial^2 T}{\partial^2 z}\right) - w_b c_b (T(r,z) - T_{art}) + P_t \qquad (1)$$

The spacing in the axial direction dz was 1mm while in the radial direction it varied from 3.6 10^{-4} mm to 0.2 mm. The computational domain was 4 cm radially and 10 cm axially. Details on the numerical scheme can be found elsewhere (Kolios *et al.* 1995; Kolios *et al.* 1994). Accurate transient temperature data are required to calculate the thermal dose (eq. 3). A comparison of the numerical solution with an analytical solution of transient heat transfer in a composite material is shown in figure 1.

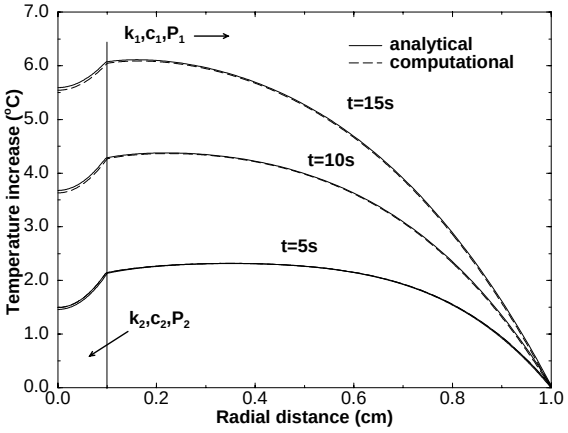

FIGURE 1: *Comparison of transient analytical and numerical solution for composite medium (simulating vessel and tissue domain) in a heated cylindrical pipe. Parameters used: inner medium (k_1=0.006 W/cm-°C c_1=4.18 and P_1=80 W/cm^3 and outer medium (k_2=0.04 W/cm-°C, c_2=4.18 and P_2=8 W/cm^3)*

The solution is for a two-layer solid with the inner (k_1, c_1 and P_1) and outer (k_2, c_2 and P_2) layer in perfect thermal contact (Ozisik 1980). A composite material was used to simulate the effects of a discrete vessel and examine how the algorithm handles conductivity discontinuities. The problem is equivalent to transient conjugated heat transfer for laminar flow in regions far form the entrance region (at a specific time interval) for which upstream axial convection has negligible influence (Yan *et al.* 1989). Lesion results with discrete vessels are not included in these simulations but will be included in future versions of this work. Heat is generated in the layers at rates P_1 and P_2. The maximum error in this example is less than 1%. Further testing with other parameter values demonstrated similar errors.

The BHTE was modeled by setting $k_{eff} = k_t$ in equation 1 and adjusting w_b to the value of perfusion of the tissue of examined. Similarly, for the ETCE model w_b is set to zero and k_{eff} assigned the value of interest. To directly compare the results, volumetric perfusion and effective conductivity were related according to the experimental data of Crezee (Crezee and Lagendijk 1990) by:

$$k_{\mathrm{eff}} = k_{\mathrm{t}}\,(1 + \alpha w_{\mathrm{b}}) \qquad (2)$$

where $\alpha = 0.12$ (ml/100g-min)$^{-1}$. Thermal properties and blood flow were assumed constant during the insonication. Ultrasonic data are given in table 1. The acoustic field intensities were calculated using the Wu

TABLE 1: List of ultrasonic parameters used in simulations.

transducer frequency (MHz):	1.7
transducer radius of curvature (cm):	14
transducer diameter (cm):	10
intensity absorption coefficient (Np/cm):	0.2
attenuation coefficient (Np/cm):	0.2

and Du model (Wu and Du 1990).

A threshold thermal dose was used to determined the extent of the lesioned tissue (Sapareto and Dewey 1984). The thermal dose can be defined as the time (t) required to produce an isoeffect at temperature T to the time (t_{43}) which would be required to produce the same effect at 43 °C:

$$t_{43} = \sum_{t=t_o}^{t_{end}} R^{T(t)-43} \Delta t$$
$$R = 0.5 \quad T >= 43^{\circ}C$$
$$R = 0.25 \quad T < 43^{\circ}C \qquad (3)$$

Tissue exposed for more than the equivalent of one hour at 43 °C was considered "lesioned". Depending on the cell type, this is roughly equivalent to 3 logs of cell kill in a typical cell survival experiment and has been shown to induce tissue necrosis *in-vivo* (Linke *et al.* 1967). The boundaries of the thermal isodose curves delineated the lesion shape and size.

RESULTS

An example of the temperature curves for different times at the focal point is shown in figure 2. A sharp temperature rise is followed by a decline immediately after the ultrasound is turned off. A significant portion of the thermal dose is delivered after the transducer is turned off thus the temperature decay is critical to the accumulated thermal dose. For the power levels used in this example the maximum temperature reached is approximately 70 °C without blood flow. For high tissue perfusions ($\sim$ 200-250 ml/100g-min, comparable to the liver), the temperature profiles are modified. The BHTE predicts a small reduction in the temperatures profiles (fig.3a). According to the ETCE however, the maximum temperature rise for high perfusion tissues reached only 40 °C (fig.3b). Therefore, for high perfusion values (such as in the liver, kidney) and according to equation 2, the ETCE does not predict the formation of lesions due to the low temperatures (and thus thermal dose) reached.

An example of a lesion formed is shown in figure 4a. The shape of the lesion agrees well with published data (Chen *et al.* 1993) and follows the intensity pattern of

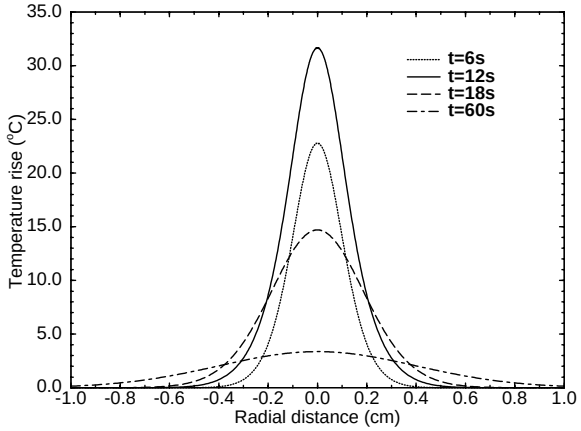

FIGURE 2: *Typical temperature profiles for a 12 second (180 W/cm^2 peak intensity) insonation at different times (no perfusion). Two minutes after the insonation the temperature has almost reached basal levels.*

the transducer. An increase of perfusion according to the BHTE reduces the lesion size (figures 4a and 4b). The reduction in size depends on the insonation time and blood flow. It is known that longer duration insonations allow the effects of both blood flow and thermal conduction to alter the temperature profiles (Billard *et al.* 1990; Hunt *et al.* 1991).

DISCUSSION

Blood flow can effect the temperature distributions and thus alter the lesion shape and size. For high perfusions, lesions are not formed according to the predictions of the scalar ETCE model. The steep temperature gradients created by the source and the high values of enhanced conductivity rapidly smear out the temperature rise. The low temperatures achieved restricted the thermal dose to non-lesioning levels. A next step of this work is to compare predictions of the thermal models with *in-vivo* data to examine if this is the case. Preliminary analysis indicates that the BHTE better fits experimental lesion data (Chen *et al.* 1993) since lesions are still formed with high flows compared to identical exposures without flow. Such analysis provides another tool for examination of thermal model validity.

The validity of equation 2 is not well established and may be valid only for the mammalian kidney cortex from which it has been derived. Dutton (1993) calculated values of effective conductivity in fixed canine livers of 0.37 W/cm-°C for a flow of 65ml/100g-min from steady state

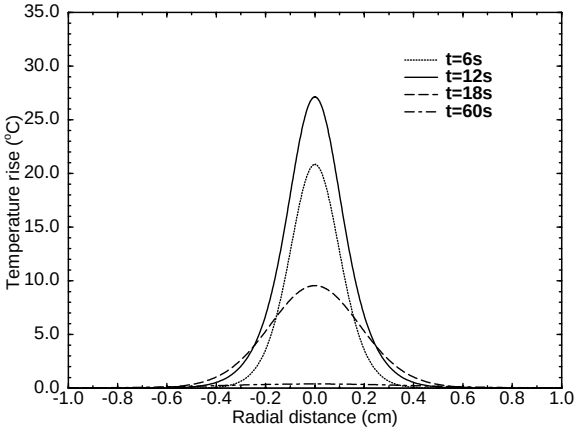

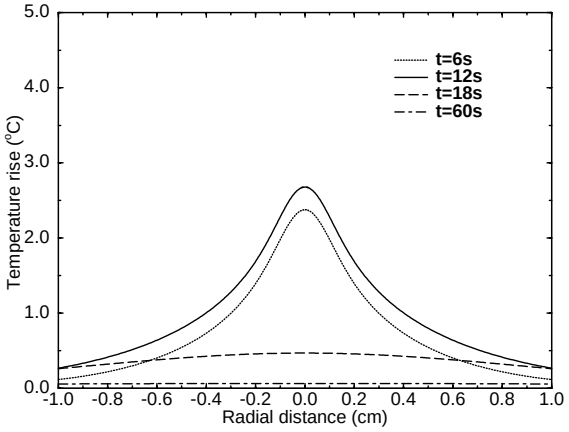

FIGURE 3: *Temperature profiles for a 12 second (180 W/cm^2 peak intensity) insonation at different times, according to a. the BHTE (perfusion was set to 0.04 g/cm^3-s equivalent to ∼240 ml/100g-min) and b. the ETCE (k_{eff} was set to 0.18 W/cm-°C). Note the different temperature scales.*

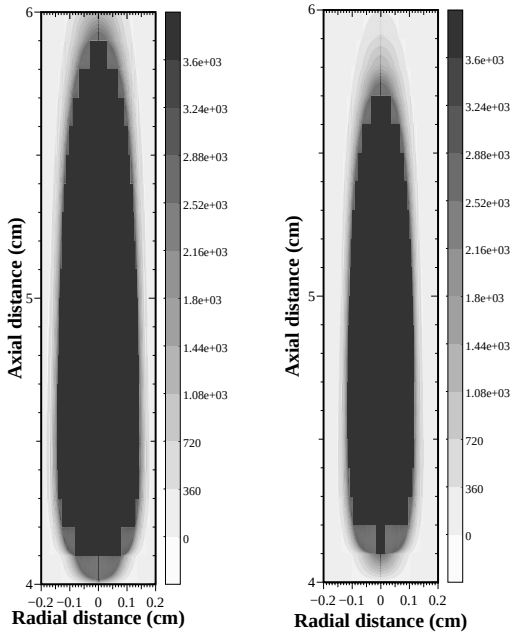

FIGURE 4: *Thermal dose contour plots for a. no perfusion b. a perfusion value of 0.04 g/cm^3-s. The thermal dose isocontour of 3600s at 43° C defines the lesion boundaries. Contour steps in 10%.*

parameter estimation of hyperthermic temperature profiles. Using a thermal diffusion probe, a 4% increase in the effective conductivity was observer in the isolated perfused rat liver system for a mean flow of 60 ml/100g-min (Bowman *et al.* 1989), however, when the experiments were performed in a fixed canine kidney the effective conductivity was estimated as 0.22 W/cm-°C for a volumetric flow rate of ∼38 ml/min. The discrepancy between the rat and dog data may be expected, since the effective conductivity depends on factors such as blood vessel diameter, length and volumetric flow, which are probably greater in the dog. Theoretical calculations may also predict high effective conductivity values: k_{eff} is estimated to increase by a factor of 11 in the cat mesentery for conditions of maximum dilation near 200μm vessels (Zhu *et al.* 1994). Therefore the high values of effective conductivity used in the simulations do not appear to be unrealistic for highly perfused tissues.

The relation between thermal dose isocontours and lesion dimensions has not been rigorously validated in an experimental setting. Equation 3 has been established for *in-vitro* cell culture systems and may not be a good predictor of thermal damage *in-vivo* at high temperatures. However, the validity of similar quantitative re-

lations has been established in animal systems in which a rise of 1°C halved the time required to induce tissue necrosis for temperatures up to 60°C (Linke *et al.* 1972; Linke *et al.* 1967). Furthermore, Damianou and Hynynen (1994) have demonstrated that thermal dose predictions match experimental ultrasonic lesions induced *in-vivo* in the rabbit thigh. Therefore, it is reasonable to assume a similar relationship for tissue lesioning.

A perfusion increase according to the BHTE reduces the size of the lesions formed due to the slight reduction in the temperatures reached (fig. 4). For highly perfused tissues such as kidney and liver, even for short exposures (~8s) lesion size can be reduced by one third. Therefore, even shorter exposure times are required to minimize the effects of blood flow. However, higher acoustic intensities are required to achieve this, and therefore phenomena such as cavitation, acoustic propagation non-linearities and non-thermal mechanisms may contribute to tissue necrosis. These effects are not well understood and cannot be, at the present time, adequately quantified (NCRP 1992). Hynynen (1991) recommended that intensities lower than 700 W/cm^2 at 1MHz be used to avoid unpredictable energy absorption due to nonlinearities or direct cytotoxicity of non-thermal effects.

CONCLUSIONS

Thermal models can be used to estimate lesion boundary formation for ultrasonic surgery and therefore can potentially be used for applicator optimization and treatment planning. Blood flow can modify lesion size. The BHTE predicts reduction in lesion size (which depends on tissue perfusion and exposure time) and the ETCE predicts that for realistic ultrasonic intensities lesions are not formed for highly perfused tissues.

ACKNOWLEDGMENTS

The authors would like to gratefully acknowledge the financial support of the National Cancer Institute of Canada and the Ontario Cancer Treatment and Research Foundation. The first author is partially supported through a University of Toronto Open Doctoral Fellowship. The authors would also like to thank Dr. Gail ter Haar for helpful discussions.

References

Arkin, H., L. X. Xu, and K. R. Holmes (1994). Recent developments in modeling heat transfer in blood perfused tissues. *IEEE Transactions on Biomedical Engineering 41*(2), 97–107.

Baish, J. W. (1994). Formulation of a statistical model of heat transfer in perfused tissue. *Journal of Biomechanical Engineering 116*(4), 521.

Billard, B. E., K. Hynynen, and R. B. Roemer (1990). Effects of physical parameters on high temperature ultrasound hyperthermia. *Ultrasound in Medicine and Biology 16*, 409–420.

Bowman, H. F., M. G. Curley, W. H. Newman, S. C. Summit, S. Chang, J. Hansen, T. S. Herman, and G. K. Svensson (1989). Use of effective conductivity for hyperthermia treatment planning. In R. B. Roemer, J. J. McGrath, and H. F. Bowman (Eds.), *Bioheat Transfer - Applications in Hyperthermia, Emerging Horizons in Instrumentation and modelling*, HTD-126 / BED-12, pp. 23–28. American Society of Mechanical Engineers.

Chen, L., G. ter Haar, C. R. Hill, M. Dworkin, P. Carnochan, H. Young, and J. P. Bensted (1993). Effect of blood perfusion on the ablation of liver parenchyma with high-intensity focused ultrasound. *Physics in Medicine and Biology 38*(11), 1661–1673.

Crezee, J. and J. J. Lagendijk (1990). Experimental verification of bio-heat transfer thoeries: measurement of temperature profiles around large artificial vessels in perfused tissue. *Physics in Medicine and Biology 35*(7), 905–923.

Damianou, C. and K. Hynynen (1994). The effect of various physical parameters on the size and shape of necrosed tissue volume during ultrasound surgery. *Journal of the Acoustical Society of America 95*(3), 1641–1649.

Dutton, A. W. (1993). *A finite element solution to conjugated heat transfer is tissue using magnetic resonance angiography to measure the in vitro velocity field.* Ph. D. thesis, University of Arizona.

Hunt, J. W., R. J. Lalonde, H. Ginsberg, S. Urchuck, and A. Worthington (1991). Rapid heating: critical theoretical assesments of thermal gradients found in hyperthermia treatments. *International Journal of Hyperthermia 7*(5), 703–718.

Hynynen, K. (1991). The threshold for thermally significant cavitation in dog's thigh muscle in vivo. *Ultrasound in Medicine and Biology 17*(2), 157–169.

Kolios, M. C., M. D. Sherar, and J. W. Hunt (1995). Large vessel cooling in heated tissues: a numerical study. *Physics in Medicine and Biology 40*(4), 477–494.

Kolios, M. C., M. D. Sherar, A. E. Worthington, and J. W. Hunt (1994). Modeling temperature gradients near large vessels in perfused tissues. In M. A. Ebadian and P. H. Oosthuizen (Eds.), *Fundamentals of Biomedical Heat Transfer*, HTD-Vol.295, pp. 23–30. American Society of Mechanical Engineers.

Lagendijk, J. J. (1990). Thermal models: principles and implementation. In S. B.Field and J. W.Hand (Eds.), *Introduction to the Clinical Aspects of Clinical Hyperthermia*, pp. 478–511. Bristol, PA.: Taylor and Francis.

Linke, C., A. Elbadawi, V. Netto, A. Roberts, and M. Russo (1972). Effect of marked hyperthermia upon the canine bladder. *Journal of Urology 4*(107), 599–602.

Linke, C. A., W. Lounsberry, and V. Goldschmidt (1967). Localized heating of tissue by electric and nonelectric means. *Investigative Urology 4*(6), 586–599.

Moros, E. G., A. W. Dutton, R. B. Roemer, M. Burton, and K. Hynynen (1993). Experimental evaluation of two simple thermal models using hyperthermia in vivo. *International Journal of Hyperthermia 9*(4), 581–598.

NCRP (1992). Exposure criteria for medical diagnostic ultrasound: I. criteria based on thermal mechanisms. Technical Report 113, National Council on Radiation Protection and Measurements, Bethesda, MD.

Ozisik, M. N. (1980). *Heat conduction.* Wiley-Interscience. pp. 303-307.

Pennes, H. H. (1948). Analysis of tissue and arterial blood temperatures in the resting human forearm. *Journal of Applied Physiology 1*, 93–122.

Roemer, R. B. (1991). Optimal power deposition in hyperthermia I.the treatment goal: the ideal temperature distribution II.the role of large blood vessels. *International Journal of Hyperthermia 7*, 317–341.

Sapareto, S. A. and W. C. Dewey (1984). Thermal dose determination in cancer therapy. *International Journal of Radiation Oncology, Biology and Physics 10*, 787–800.

ter Haar, G., I. Rivens, L. Chen, and S. Riddler (1991). High intensity focused ultrasound for the treatment of rat tumours. *Physics in Medicine and Biology 36*(11), 1495–501.

Weinbaum, S., L. M. Jiji, and D. E. Lemons (1984). Theory and experiment for the effect of vascular microstructure on surface heat transfer -part I: Anatomical foundation and model conceptualization. *Journal of Biomechanical Engineering 106*, 321–330.

Wu, J. R. and G. H. Du (1990). Temperature rise in a tissue-mimicking material generated by unfocused and focused ultrasonic transducers. *Ultrasound in Medicine and Biology 16*(5), 489–498.

Yan, W. M., Y. L. Tsay, and T. F. Lin (1989). Transient conjugated heat transfer in laminar pipe flows. *International Journal of Heat and Mass Transfer 32*(4), 775–777.

Zhu, L., D. E. Lemons, and S. Weinbaum (1994). A new approach for predicitng the enhancement in the effective conductivity of perfused tissue due to hyperthermia. In L. Haynes and R. B. Roemer (Eds.), *Advances in Heat and Mass Transfer in Biological Systems*, HTD-288, pp. 37–43. American Society of Mechanical Engineers.